Published at the 2nd Worldwide SYSNOISE Users Meeting, Leuven, June 19-21 1995, Paper II.5.

Calculation of sound radiation from sources, characterized by the equivalent power volume velocity method

F. Augusztinovicz, F. Penne and P. Sas

Katholieke Universiteit Leuven, Dept. of Mechanical Engineering
Celestijnenlaan 300B, B-3001 Leuven, Belgium
e-mail : *Fulop.Augusztinovicz@mech.kuleuven.ac.be*

1. Introduction

The paper reports on an attempt to implement the equivalent power volume velocity (EPVV) method, developed by J. Verheij *et al.* originally for partial source identification purposes [1], for the numerical calculation of sound fields. This novel source characterization method describes sound sources by determining a set of substituting fictitious monopole sources, assumed to be uncorrelated and radiating power equal to that of the source to be described. As a usual result, rather complex real-life sources can be substituted by a few tens of equivalent sources. The great advantage of the method is that the obtained sound source characteristics are insensitive to significant changes of the acoustic environment (e.g. caused by the presence of a close-fitting noise control enclosure) and the method can be easily adapted for transient sound sources as well.

Although lacking phase information, its simplicity and proven robustness makes this technique an attractive approach for numerical calculation of sound fields radiated from mechanical structures, too. From the point of view of our investigations aimed at adopting and developing effective yet affordable calculation methods to predict the efficiency of truck engine enclosures [2], the tremendous data reduction potential of the method was considered an essential asset. (Even though successful calculations have already been reported as early as 1988 [3], the vibration characteristics of complex sources such as fully equipped heavy diesel engines are difficult, if not impossible, to characterize by using any other technique as detailed as it is required for wide frequency range numerical calculations.) This report summarizes the applied methods and discusses some calculation and experimental verification results, obtained for a simple engine mock-up surrounded with a partial close-fitting enclosure and for a more realistic engine simulator.

2. Source substitution by means of the EPVV method

The surface of the investigated source is subdivided into j areas, each S_j considered as a partial source. The acoustic power P_j, radiated from these partial sources is determined by means of sound intensity measurements, scanned along contiguous parts of an appropriately selected closed measurement surface around the free source.

The basic idea of the method is that the surface vibration of the partial sources S_j is substituted by a few uncorrelated monopoles, located at the source surface and radiating the same total power P_j like the original surface. The source strength of these monopoles is calculated on the simplified assumption that the monopoles radiate into half space backed by an infinite, rigid surface, corresponding to a radiation resistance which is twice of that of the free field. Thus, assuming that the source strength of the n_j monopoles along the partial surface are equal, one can calculate the equivalent source strength Q_{ji} of the i-th monopole from the formula

$$Q_{ji} = \sqrt{\frac{P_j}{n_j}\frac{2\pi c}{\rho\omega^2}} \qquad (1)$$

The numerical implementation of these ideas for BEM radiation calculations is quite straightforward. The only amendment is that instead of placing point sources on the source surface assumed to be rigid (which would need an unnecessarily fine mesh behind the monopoles), certain elements of the source mesh itself are selected to be equivalent sources. Normal velocities derived from Eq.(1) are imposed as velocity boundary conditions on these elements, while zero velocities are attributed to the rest of the source surface.

Besides the appropriate subdivision of the full source and determination of the necessary number and locating of the equivalent monopoles (which are common issues for all applications of the method), a specific problem of the numerical implementation is the matter of phase. The EPVV method is constrained to power quantities and by doing so, the assumption of uncorrelated equivalent sources is inevitable. Although a similar implementation by using narrow-band functions was also reported [4], most calculations and verification experiments have so far been performed in third-octave bands only [2]. On the contrary, the presently available SYSNOISE versions are based on a sinusoidal source description, corresponding to a fully coherent source for discrete frequencies. This contradiction seems to have been solved by using random phasing of the sources along with third-octave band averaging.

3. Numerical simulations of the sound radiation from a simple source

3.1. Construction and vibration characteristics of the mock-up

The various possibilities of source modelling and sound field calculations will be discussed first on the example of a simple mechanical mock-up developed at K.U.Leuven, the vibrational and sound radiation behaviour of which is well known from earlier investigations [5,6]. The applied source mock-up is a welded steel box of dimensions 400 mm x 300 mm x 150 mm, thickness 5 mm, with one bulkhead inside. Its vibration characteristics were measured in terms of acceleration per input force FRFs in 296 measurement points, on the basis of which experimental modal and running mode analyses were performed. It was found that the structure is lightly damped and the first 10 structural modes lie between 180 Hz and 860 Hz, thus the modes are well separated.

Some typical operational deflection shapes of this structure, determined at three frequencies selected close to modal frequencies are shown in Fig. 1. (For the sake of clear visualisation, only the two larger sides of the box are shown). The surface vibration at 495 Hz, Fig. 1a., is characterized by a clear in-phase motion of the structure (in the sense that the surface elements are moving towards the acoustic fluid in the same time; this motion will be referred to as *con-phase* motion below) while Fig.1b. shows a simple out-of-phase vibration pattern at a frequency only 20 Hz higher (this sort of surface vibration will be denoted as *anti-phase* motion). Eventually, a more complicated vibration pattern observed at 100 Hz frequency is shown in Fig.1c.

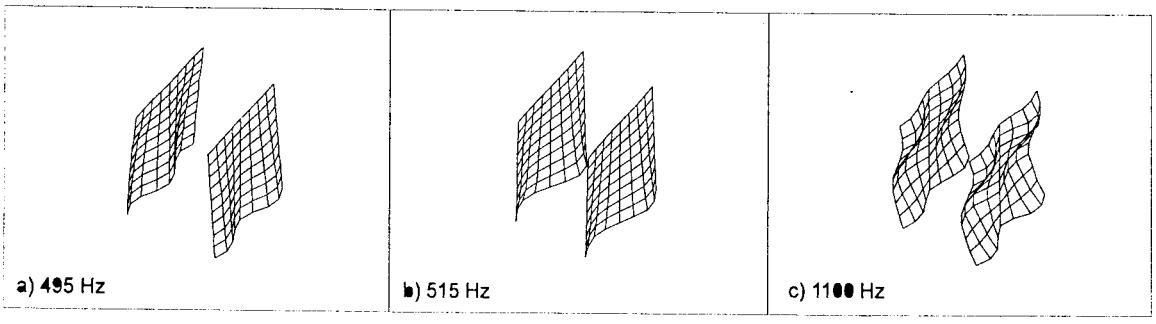

Fig. 1 : Operational deflection shapes of the KUL engine mock-up

3.2. Sound radiation simulations under free-field conditions

The measured vibration data were used to predict the sound radiation of the mock-up in various, more "traditional" ways [6]. The best agreement with verification experiments was found when the vibration input was used in form of directly imposed velocity boundary conditions by using the GENERATE command of SYSNOISE.

In order to obtain input data for the EPVV method, the radiated sound power of the mock-up was determined along a rectangular, hypothetical measurement surface stretched just above the reflecting plate of the support and at a distance of 75 mm from the source. As shown in Fig. 2, the source surface was subdivided into 14 subareas. Third-octave band sound intensity values were measured in front of these subareas, scanned along the corresponding parts of the measurement surface while the structure was excited by an electrodynamic shaker from behind.

In the course of the first EPVV trials the measured sound powers were assumed to have been radiated from one single equivalent source per subarea (also denoted in Fig. 2.), and this at one single frequency only. The obtained sound pressure pattern is shown along a special H-form field point mesh which enables one to observe the variation of the acoustic variables both along the surface of the source (the close edge of the field point is 5 cm apart from the source) and away from it.

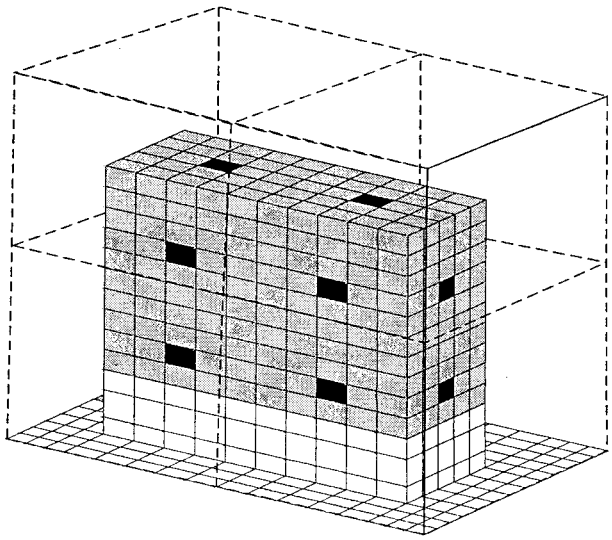

Fig. 2 : Substitution sources and measurement subareas on the KUL engine mock-up

In Fig. 3. the obtained sound pressure patterns are compared for the surface velocity calculation and for the EPVV method (using zero phase for all substitution sources) for 495 Hz. As one can see, the sound pressure pattern is quite similar to the calculation based on the measured surface velocities.

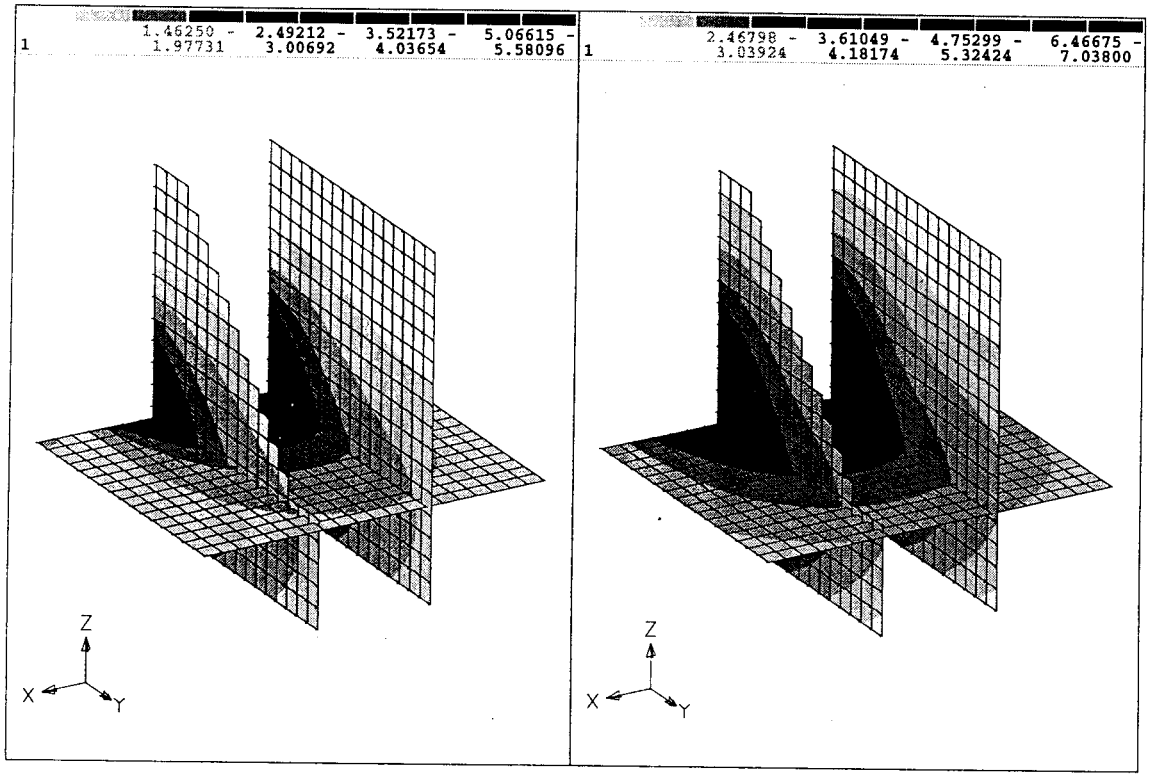

Fig. 3. : Comparison of simulated pressure patterns for source vibrations as shown in Fig. 1a. Left side : source described by full data set, right side : source described by the EPVV method

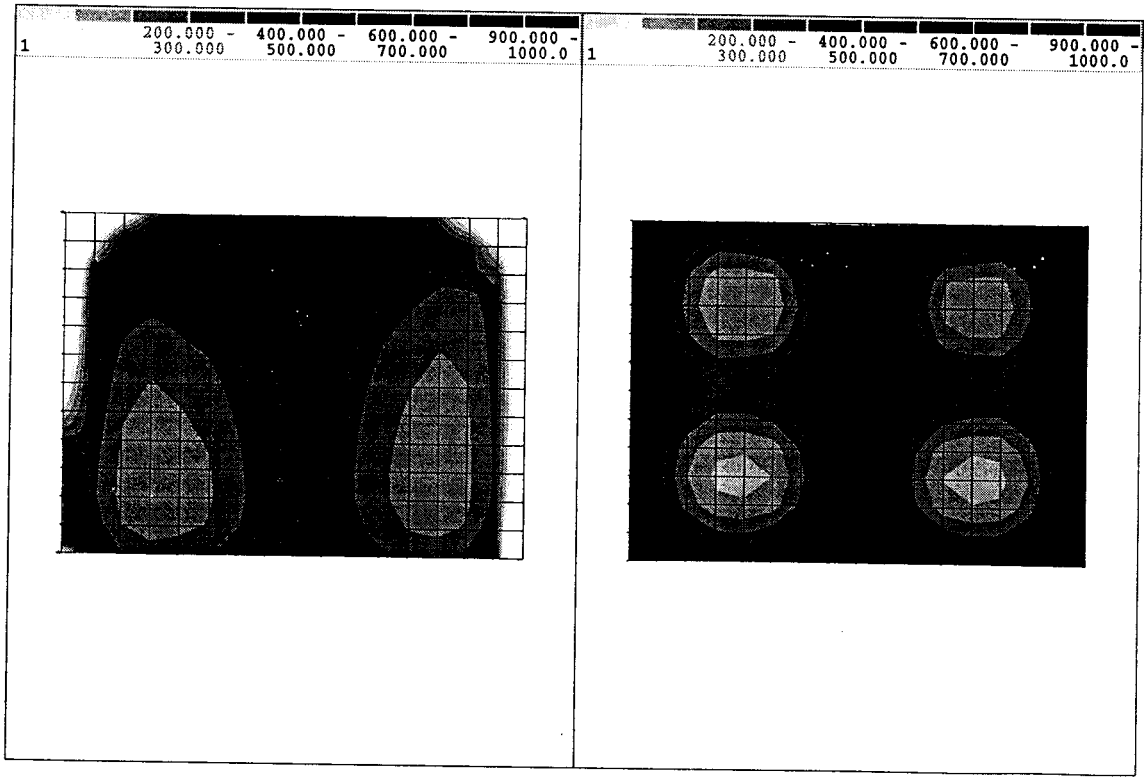

Fig. 4. : Comparison of simulated radiation resistance distributions at a distance of 4 cm from the mock-up, for source vibrations as shown in Fig. 1a. Left side : source described by full data set, right side : source described by the EPVV method

A better insight can be gained into the behaviour of the various simulations if the (locally varying) radiation resistances and the (overall) radiation efficiencies are also compared. According to the basic assumption of the method, the power P_j radiated from surface S_j can be calculated from the sound field parameters taken along S_j as follows:

$$P_j = \frac{1}{2}\mathrm{Re}\int_{S_j} p v^* \, dS = \frac{1}{2}\int_{S_j} |v|^2 R \, dS = \frac{1}{2}\sum_{i=1}^{n_j} |v_i|^2 R_i \qquad (2)$$

where p and v are (complex) amplitudes, R is radiation resistance, v_i is the normal velocity and R_i is the radiation resistance on the i-th substitution source element. The radiation efficiency can be expressed as follows:

$$\eta = \sum_j \int_{S_j} |v|^2 R dS \; / \; \rho c \sum_j \int_{S_j} |v|^2 \, dS \qquad (3)$$

Fig. 4. shows the spatial variation of the radiation resistance along a field point mesh selected at 4 cm distance from the source. Unlike the pressure patterns, the near-field impedance calculations show clear differences in the source distribution. More important is however, that the obtained radiation resistances just in front of the substitution sources (where the velocities are nonzero) are lower than that of the fully vibrating source. Lower radiation load results in lower radiation efficiency as well, summarized in Table 1. All these imply that the source strength of the equivalent sources should be very high with respect to the real surface velocities, for two reasons: not only the much smaller vibrating surface but also the lower radiation load has to be compensated for.

Table 1. *Comparison of the radiation efficiencies (in %) of various simulations*

Frequency Hz	Kind of mode shape	Simulation based on			
		measured surface velocities	EPVV with 0^0 phasing	EPVV with 180^0 phasing	EPVV with random phasing
495	con-phase	40	3.3		2.2
515	anti-phase	21		4	2.3
1100	complex	55			8.1

The vibration pattern of Fig. 1b. can obviously not be correctly simulated by equivalent sources having the same phase. Instead, the EPVV calculation was performed with 180^0 phase values attributed to the source elements on opposite sides of the source. The resulting pressure pattern, Fig. 5, shows a more expressed deviation that it was the case for the con-phase pattern. The differences in the radiation resistances (not shown due to space limitations) are also higher than in the con-phase case, though the deviation in the radiation efficiency is lower.

Eventually, the results of the EPVV simulation are shown and compared in Fig. 6. for 1100 Hz. Facing a more complicated vibration pattern, random phasing of the equivalent sources was attempted this time, resulting in more satisfactory results than before. The obtained pressure patterns are reasonably similar, the radiation resistances show more uniformity and the ratio of the obtained radiation efficiencies is relatively low, too. These results suggest that as the vibration complexity of the source increases (i.e., as the basic assumption of the method is better approximated), the accuracy of the numerical sound field simulation is also improved.

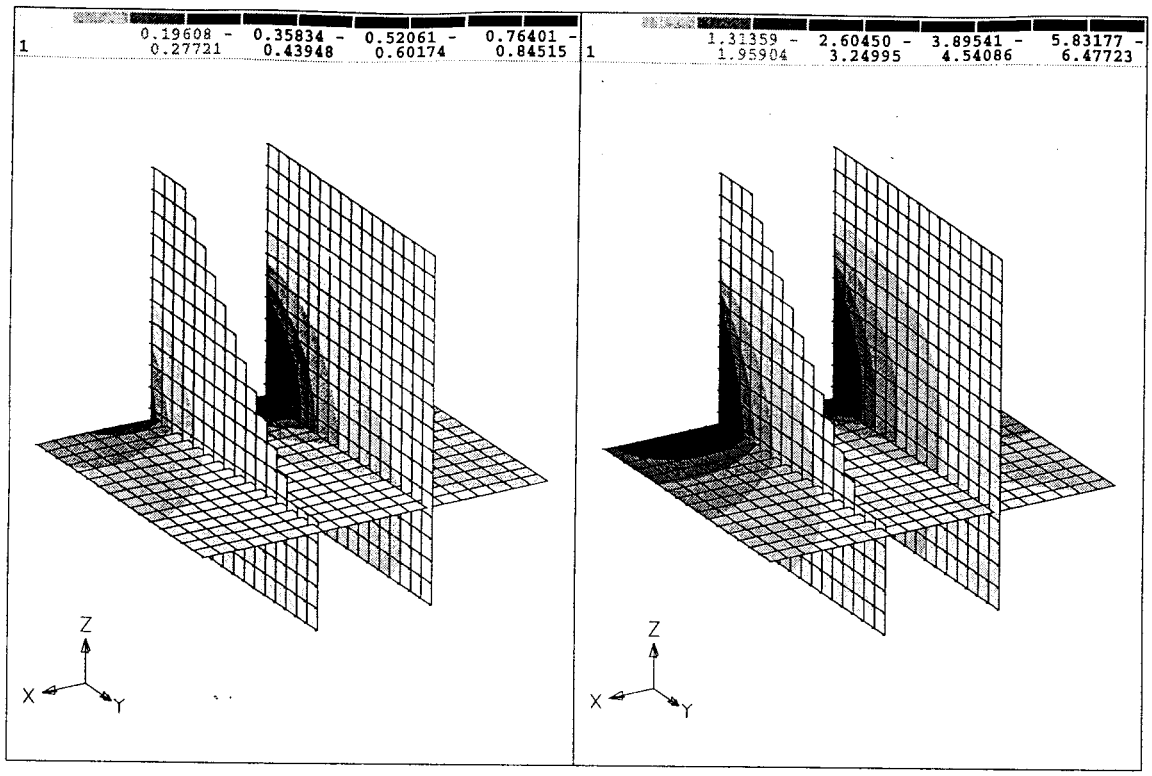

Fig. 5. : Comparison of simulated pressure patterns for source vibrations as shown in Fig. 1b. Left side : source described by full data set, right side : source described by the EPVV method

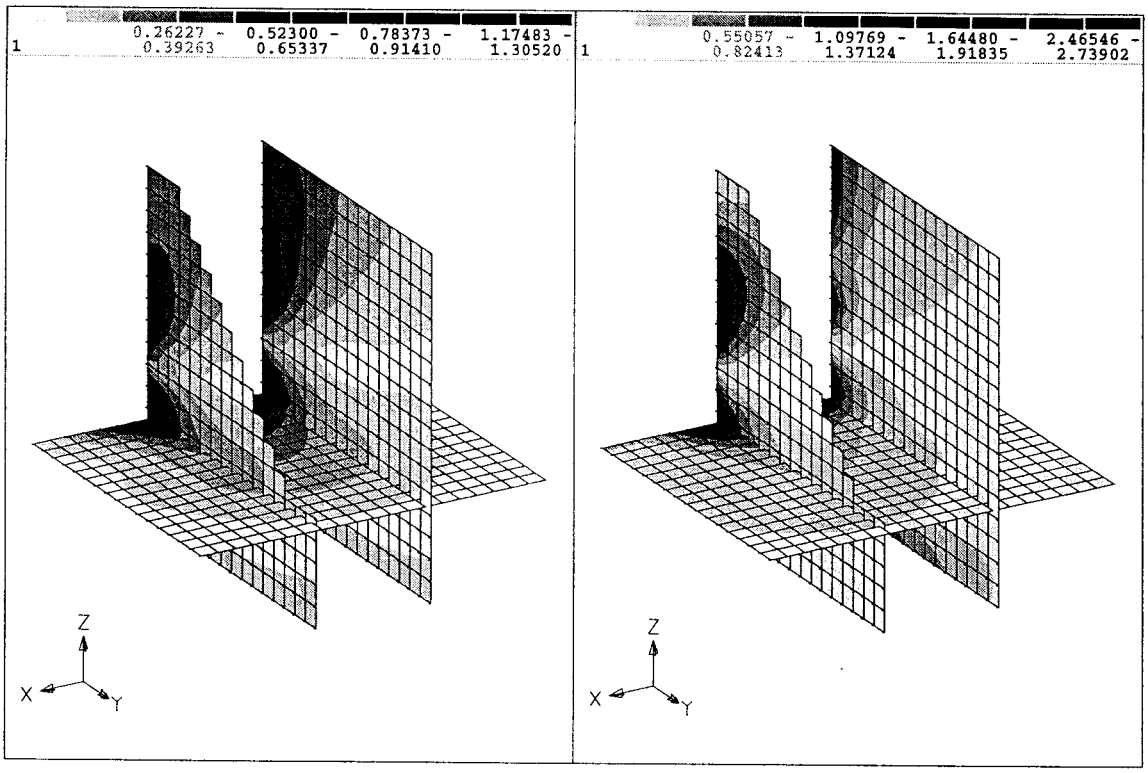

Fig. 6. : Comparison of simulated pressure patterns for source vibrations as shown in Fig. 1c. Left side : source described by full data set, right side : source described by the EPVV method

3.3. Simulation of the Insertion Loss of a tunnel-type shield

Starting from experiences of the first calculations, the insertion loss of a plate and a tunnel-type shield was also calculated by the EPVV method. The number of equivalent sources per subarea was still kept one, but the calculations were performed for more frequencies. To be more specific, we have assumed that the sound power measured in each third-octave band is distributed equally among 4 (or 8) substitution sources operating at randomly chosen frequencies within the band. The calculations were performed by randomly chosen phases of the equivalent sources. The intensities were calculated and averaged along a plane field point mesh at 0.5 m distance from the source for each frequency, and the obtained intensities were eventually summed. The simulation was conducted both for the free-field case and with the shield in place. The insertion loss of the shield was then calculated in the classical way.

The predicted free-field sound intensity spectra are shown in Fig. 7. along with their measured counterpart. Apart from a systematic deviation ranging from 1.5 dB to 3 dB, the prediction is quite reasonable. Similar systematic error was encountered in the estimation of the intensities with the plane sound shields, resulting in a rather good prediction of the Insertion Loss as shown in Fig. 8. Doubling the number of the averaged frequencies did not improve the accuracy essentially.

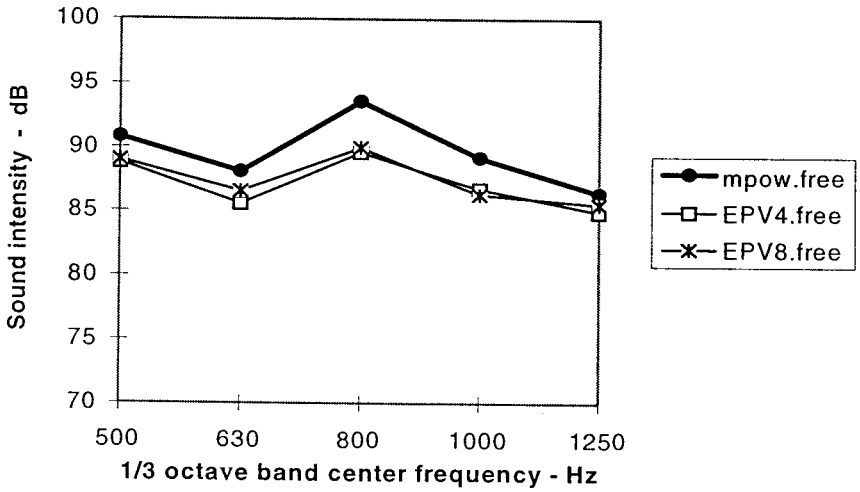

Fig. 7. : Prediction of the sound field of the KUL engine mock-up under free-field conditions along a field point mesh. Thick line : measurement, thin lines : EPVV estimations

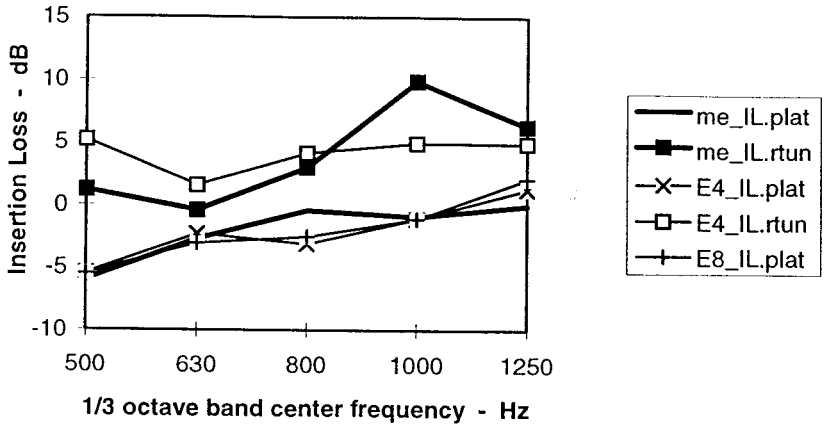

Fig. 8. : Predictions of the Insertion Loss of a plate and a tunnel-type sound shield. Thick lines : measurement, thin lines : EPVV estimations

Although the tendencies can still be identified, the prediction of the efficiency of the tunnel-type shield is less accurate with errors between -5 and +4 dB. However, one has to note here that the maximum deviation is most probably caused by one single calculation at an irregular frequency.

4. Simulation of the free-field radiation from a real-size engine simulator

A full-size engine simulator was developed in the TNO Institute of Applied Physics in the Netherlands by J.W. Verheij and his colleagues [1]. This source is also a steel parallelepiped but of dimensions similar to a real engine (1000 mm x 600 mm x 740 mm, wall thickness 6 mm). The structure is stiffened from inside along the side walls, an oil sump of a truck engine is installed from below and a thinner steel plate simulates the valve covers of a real engine on top. The excitation is ensured by a strong electrodynamic shaker built inside, driven by a swept sine electric signal. The engine simulator was placed in a semi-anechoic chamber of TNO. Among others, both near-field intensities (along 10 subareas around the source) and far-field sound pressures in two microphone positions were measured.

These measurements were used both as input data and as verification tools in our numerical calculations. Five simulations have been performed:

- *a)* with one equivalent source per subarea and three frequencies per third-octave band;
- *b)* as *a)* but with different spatial selection of the substituting elements;
- *c)* with five equivalent sources per subarea and three frequencies per third-octave band;
- *d)* with five equivalent sources per subarea and six frequencies per third-octave band, and eventually
- *e)* with five equivalent sources per subarea and nine frequencies per third-octave band.

The obtained sound pressure predictions for one of the far-field microphone positions (at app. 1.9 m distance from the source and 1.2 m height above the sound reflecting floor of the measuring room) is compared to the measured values for the third-octave bands between 315 and 800 Hz in Fig. 9. (The applied structural mesh did not allow to perform calculations above 900 Hz. Even so, the size of the model was 1930 elements, resulting in typical calculation times of app. 50 minutes for one frequency on a HP 9000/710 Type workstation.)

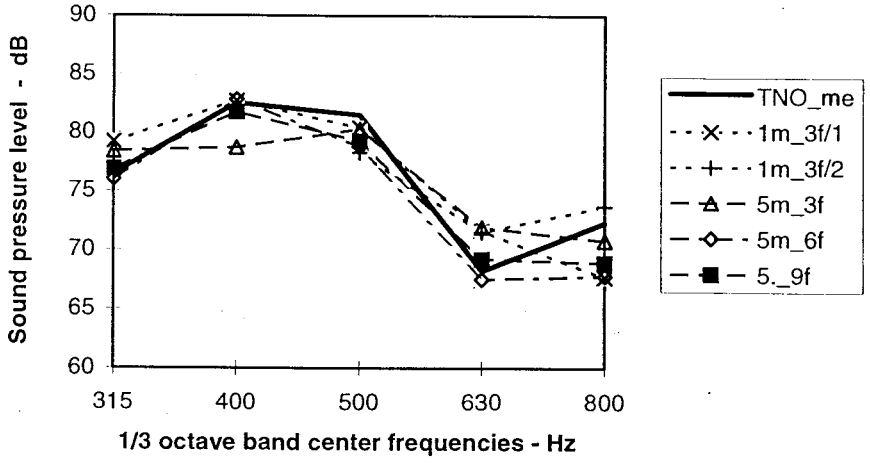

Fig. 9. : Prediction of the TNO engine mock-up under free-field conditions in a single measurement point. Thick line : measurement, thin lines : EPVV estimations

Even though the spatial resolution of the simplest model (case *a)*) is very rough, the obtained estimation is already quite satisfactory, in spite of the fact that this prediction refers to

one single field point instead of averaging along any surfaces. The accuracy, especially in the lower frequency bands, are generally improved by using more monopoles per subareas but for certain frequencies it can be worse, too. As expected however, the best results have been obtained by using the most sources and most frequencies: the error ranging from 0.5 to 2 dB except for the highest band where it increases up to 3.4 dB.

5. Summary and conclusions

The sound field around a simple and a more complicated engine mock-up was calculated by means of the Equivalent Power Volume Velocity method. The results were compared to predictions based on detailed surface velocity measurements and/or to direct measurements.

The obtained results seem to be quite promising. The estimations of the absolute field descriptors sometimes show a small systematic deviation. Nevertheless, the Insertion Loss predictions are unbiased and burdened with errors which are not higher than those obtained by using much more detailed source descriptors. The most important and attractive feature of the technique is that the more complex the source is, the more accurate results can be obtained. Note that the final validation of the technique on various real-life engines are in progress.

6. Acknowledgements

The authors express their special thanks to Prof. J. W. Verheij for his kind approval to perform and publish numerical calculations with TNO data. The valuable discussions with Prof. Verheij, Prof. F. J. Fahy, Mr. J.-L. Migeot and other partners of the PIANO project are also highly appreciated. The project was supported by the Directorate-General for Science, Research and Development of the Commission of the European Union.

7. References

1. J. W. Verheij, A.N.J. Hoeberichts and D.J. Thompson, "Acoustical source strength characterization for heavy road vehicle engines in connection with pass-by noise."
Proc. 3rd Int. Congress on Air- and Structure-Borne Sound and Vibration (Ed. M.J. Crocker), June 13-15 1994, Montreal, Vol. I. 647-654. p. (1994)
2. BRITE-EURAM Project No. 5414: New pass-by noise optimization methods for quiet and economic heavy road vehicles (PIANO)
3. A. F. Seybert and R. Khurana, "Calculation of the sound intensity and sound radiation efficiency of structures from vibration data."
Proc. 6.th Int. Modal Analysis Conf., Kissimmee, Vol. I. 302-308.p. (1988)
4. J. Zheng, F.J. Fahy and D. Anderton: "Application of a vibro-acoustic reciprocity technique to the prediction of sound radiated by a motored IC engine".
Applied Acoustics , **42** 333-346.p. (1994)
5. F. Augusztinovicz, P. Sas and F. Penne: "Comparison and verification of experimental and numerical models for the prediction of the efficiency of engine noise shields".
Proc. 1995 SAE Noise and Vibration Conference, Traverse City, May 1995, Paper #95NV70
6. F. Penne, F. Augusztinovicz, L. Cremers and P. Sas: "Prediction of engine shield performance by means of a hybrid experimental/numerical approach."
Proc. 2nd Worldwide SYSNOISE Users Meeting, Leuven, 19-21 June 1995.
7. F.P. Mechel, "Notes on the radiation impedance, especially on piston-like radiators".
J. Sound Vib., **123** (3) 537-572. p. (1988)
8. F. Augusztinovicz, P. Sas and F. Penne: "Sound radiation from structures in the presence of close-fitting sound shields."
Proc. Noise-Con 94, Fort Lauderdale, May 1-4 1994, 219-224. p. (1994)